Analysis and Design of a Wing Trailing Edge Mounted Over-The-Wing Distributed Propeller Propulsion system

Veldhuis, Leo; Khajehzadeh, Arash

DOI
10.2514/6.2019-3692

Publication date
2019

Document Version
Final published version

Published in
AIAA Aviation 2019 Forum

Analysis and Design of a Wing Trailing Edge Mounted Over-The-Wing Distributed Propeller Propulsion system

Leo Veldhuis* and Arash Khajehzadeh†
Delft University of Technology, Kluyverweg 1, 2629 HS Delft, The Netherlands

In this paper we address a preliminary assessment of the aerodynamics and performance effects of a propeller based distributed propulsion that is positioned at the trailing edge of a wing. The proposed layout is a potential candidate for the application of hybrid-electric propulsion in a green aircraft design that is currently being developed in a TU Delft project. Based on experimental results that were obtained earlier during two experimental test campaigns in a low speed windtunnel, a ducted propeller-wing combination, obtained by adding a secondary wing (duct) above the propeller, was investigated and optimized using a Euler based optimization framework. From the provisional results is was found that the ducted propeller positioned close to the trailing edge may beneficially support a high overall propulsion efficiency attaining high system lift to drag values and high propeller efficiency for a typical medium range aircraft when the duct is properly adapted by shape optimization of the secondary wing.

I. Introduction

RECENT studies on novel aircraft configurations employing distributed propulsion that are based on a hybrid-electric energy source, have shown interest in multiple fans mounted on the wing [1–3]. Designs in which use is made of leading edge mounted tractor propeller design may have interesting performance characteristics although engine failure may have serious detrimental effects on the stall behaviour. Moreover, a non-negligible noise penalty may be associated which such designs [4]. To overcome these problems a wing trailing edge (TE) mounted distributed propulsion (DP) system is being investigated at Delft University as part of an EU-funded framework program. In this case utilization of an additional shielding (duct) positioned directly over the distributed propellers is envisioned to:

- increase the overall propulsive efficiency of the design
- to reduce the noise radiation to the environment.

Fig. 1 shows a typical design that relies on this wing TE mounted distributed propulsion system. The overall performance of this design was earlier addressed by Hoogreef et al [5] in comparison study for hybrid-electric driven aircraft concepts. In that particular study the application the propulsive empennage was considered to have detrimental effects on aircraft weight, yet the application of wing distributed propulsion seems attractive to be applied in novel designs.

II. Background

The application of trailing edge based propeller propulsion has been investigated both experimentally and numerically and was discussed in several references. Isyanov, et al [6] state that "the application of DP systems on long range airplanes is a new engineering solution, which may allow meeting the future advanced efficiency goals." The study focuses on BLI as well as DP systems, and it shows the possibilities

*Professor, Faculty of Aerospace Engineering, Kluyverweg 1, 2629 HS, Delft, The Netherlands, Member AIAA
†MSc student, Faculty of Aerospace Engineering, Kluyverweg 1, 2629 HS, Delft, The Netherlands

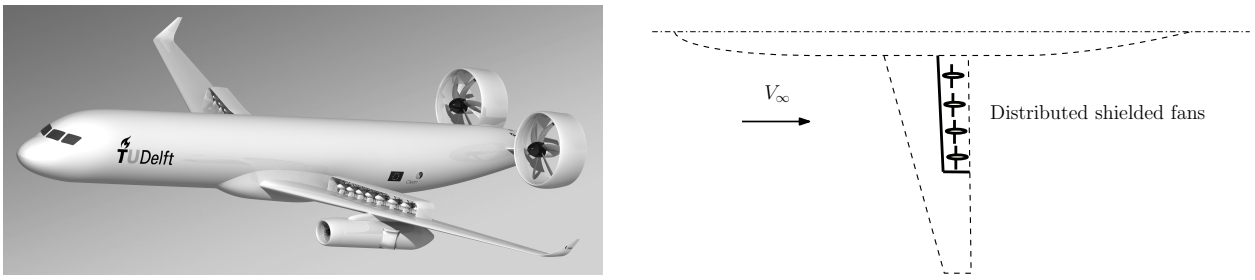

Figure 1 Artist impression of a next generation medium range aircraft study equipped with a distributed propulsion system and a propulsive empennage [5] (left) and a conceptual sketch of the investigated trailing edge located shielded propeller system (right).

and opportunities that DP concept provides. Reynolds et al [7] conducted a wind tunnel test on a scaled model of the NASA generic transport model, which utilizes two generators per wing with an addition of four fans. Their flexible wing distributed propulsion aircraft concept achieved a 4% improvement in lift to drag ratio over a mission profile consisting of a minimum fuel climb, minimum fuel cruise, and continuous descent. Catalano[8] studied the influence of a pusher propeller on the wing performance. He shows that the propeller induced flow over the wing's surface increases lift and pressure drag of the wing. Moreover, propeller inflow also delayed transition showing laminar flow over a smooth wing up to 80% of the chord. In studies conducted by Muller et al [9, 10] a propeller was positioned in an over the wing (OTW) fashion introducing a local spanwise drag coefficient that was smaller than that of the clean wing. The effect was ascribed to the propeller induced positive angle of attack over a large portion of the wing. Moreover, the lift performance and overall efficiency at low Mach numbers seemed higher than that of a tractor propeller configuration. Muller et al suggested that OTW configuration might be advantageous compared to pusher, tractor or channeled wing configurations. At the same time they recommend to investigate the influence of the wing shape on the aerodynamic performance in cruise condition where the lift to drag ratio is more sensitive to the drag coefficient. At Delft University of Technology, Luijendijk [11], Veldhuis[12] and Marcus et al [13] investigated the consequence of the OTW based propeller and they showed that the chordwise position of the propeller (with respect to the main wing) affects the performance of the design significantly. These cases gave valuable insight in the key interaction effects of a trailing edge shielded propulsion (TESP) system and provided validation data for subsequent numerical design and CFD-analysis studies.

Photographs of the two test setups that were used earlier are presented in fig. 2[11, 13]. Test #1 consists of an unducted propeller that is positioned over the wing at different chordwise locations and a fixed spanwise position. Test #2, in which the same propeller as that of Test #1 was positioned over an high performance (laminar) wing, is more representative of a modern aircraft wing. It contains an efficient single slotted flap which was used to investigate the effects of flap-slipstream interaction and boundary development under the influence of the propeller induced pressure field [13].

In Test #1 campaign, the propeller streamwise position with respect to the wing was changed and the key effects on lift and drag as well as the propeller performance were obtained. Fig.3a shows a typical effect that the propeller induces on the wing lift when the chordwise position is varied. Due to the flow entrainment into the slipstream tube and the suction forces that result from the close proximity of the wing, the lift increases when the propeller is positioned close to the surface. A peak value is reached around a propeller position around $x_p/c = 0.8$. The effect on the wing drag is presented in fig. 3b. Due to increased angle of attack by the propeller the drag becomes negative with minimum values found around $x_p/c = 0.8$.

The effect of a single propeller on the local lift and the development of the propeller was investigated in Test #2. An example of some data obtained is presented in fig. 4 and fig. 5. Again significant effects were found for the OTW position of the propeller.

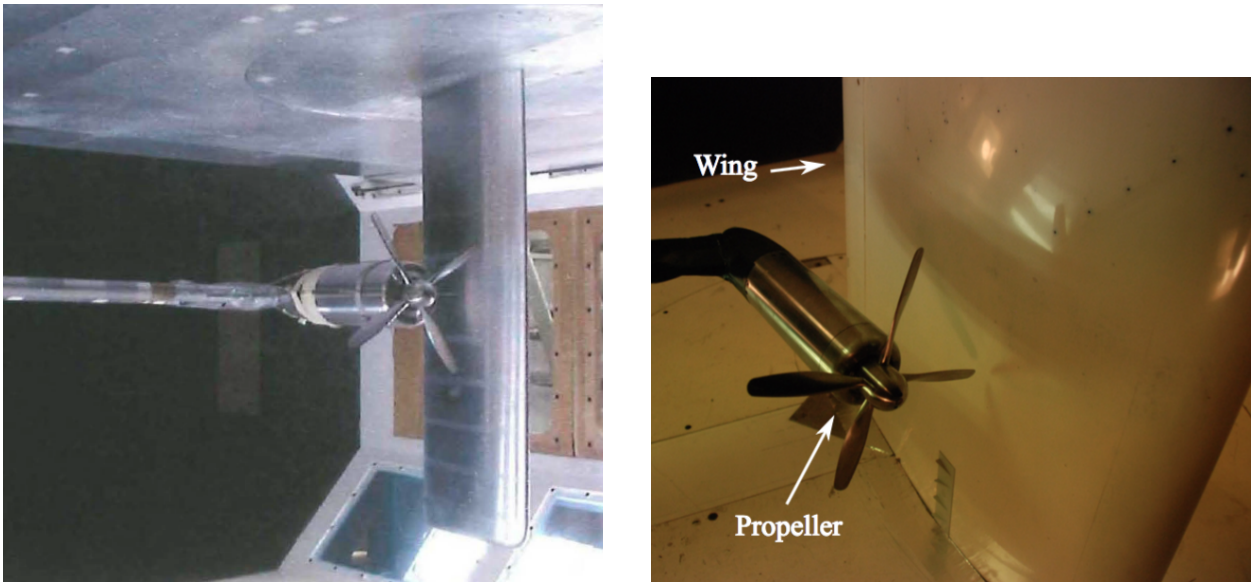

Figure 2 Low speed windtunnel Tests #1 (left, APROPOS) [11, 12] and #2 (right, X400) [13] on over-the-wing propeller configurations used for analysis of key interaction effects and the validation of CFD calculations.

For this particular experiment also a low fidelity approach was considered in which the wing effect on the propeller was investigated [13]. These data were proven to be helpful in better understanding the effect of the distance between the propeller and the wing on the propeller performance and to select an appropriate model for the actuator disk that was used in the numerical optimization study later-on. The approach in that numerical study is based on a Blade Element Model (BEM) adapted for non-uniform inflow combined with a surface singularity (panel) method.

With the propeller installed above the wing and in close proximity, the wing induced pressure field changes the propeller inflow field significantly. However, this non-uniform inflow field deteriorates the propeller's performance which may have detrimental effects of the system's overall propulsive efficiency. Fig. 7 shows typical changes to the propeller inflow field when a propeller with a tip clearance, t_{tip}, and diameter, D_p, is installed is installed at location, x_p, above wing of infinite span and chord length, c, as sketched in Fig. 6. In this case the field data are for a symmetrical NACA0012 and a cambered NACA4420 airfoil respectively.

As a result of this wing induced flow field the propeller characteristics are changed, an example of which is presented in Fig. 8. In this case the effect is shown for the propeller wing configuration of Experiment #2 with the propeller located at $x_p = 0.342c$ above the wing at a tip clearance of $t_{tip}/c = 0.01$. The thrust coefficient of the propeller, defined by $C_T = T/(\rho n^2 D^4)$, was calculated from a BEM model that was adapted to take into account non-uniform inflow in the propeller plane. The effect of wing proximity is recognizable. Due to the increased flow speed above the wing the effective advance ratio, $J_{eff} = V_{eff}/nD_p$, that is based on the local effective flow speed, V_{eff}, at constant propeller speed, becomes higher which leads to a decreased thrust coefficient. Beyond $J = V_\infty/nD_p = 0.9$ the thrust even becomes negative whereas in the situation without propeller still a positive thrust was produced. Obviously, apart from the changes in thrust at constant propeller speed , the propeller efficiency, η_p, is affected. These effects need to be taken into account in any OTW propeller design study.

A duct (or secondary wing) installed above the propeller may correct this flow to become more uniform and would also allow the flow speed at the location of the propeller disk to be lower than the undisturbed flight speed. As a consequence such a system may prove to have overall increased lift performance and

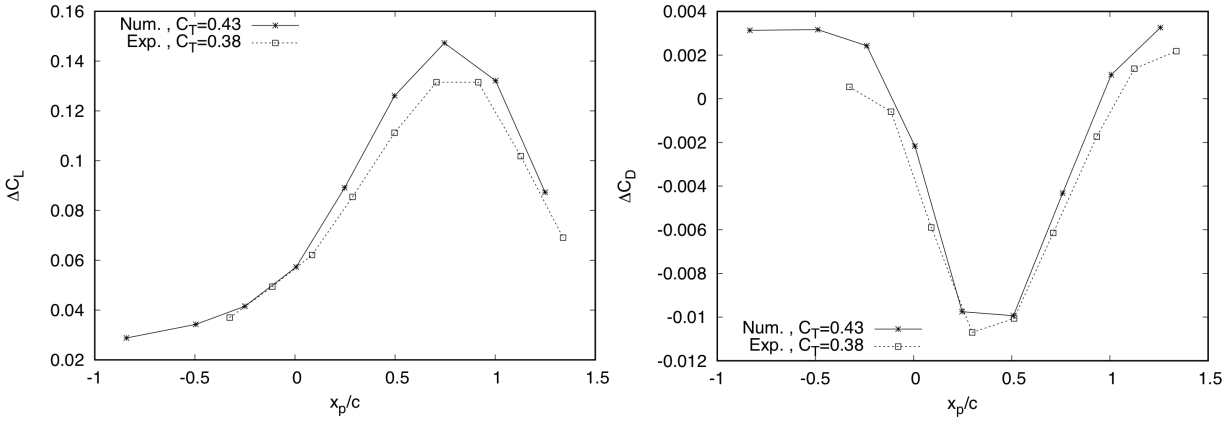

(b)

Figure 3 Lift and drag coefficient versus streamwise propeller position for an angle of attack of $\alpha = 4.2^0$ at $V_\infty = 30m/s$ from APROPOS test #1. Comparison of experimental and numerical values. Data from Luijendijk[11].

higher propulsive efficiency when designed properly. Earlier, Hongbo et al[15] discussed potential beneficial interference between a wing and a secondary wing in an over the wing fashion. In the subsequent sections the approach to analyze configuration consisting of main wing, secondary wing (straight duct) and propeller is addressed and results from an optimization study are discussed.

III. Numerical approach

A. Propulsion system layout

The DP system analysis in this study is based on the flow conditions encountered for a typical reference aircraft. In this case the ATR72 was considered to provide data on flow speed and propulsion power required in cruise condition. The model considered in this research is one of the engines in a DP array (closest to Mean Aerodynamic Chord, see fig. 9). The problem was simplified by assuming that the aerodynamic features of the considered part are periodically reoccurring in the rest of the engines. As such the calculation and the analysis effort is significantly reduced. Applying periodic boundary conditions is deemed acceptable to model at least 3 neighboring propellers since the reference aircraft has a very small quarter chord sweep angle of 3^0 and a moderate taper ratio of 0.6 [14].

The model's potential improvements were obtained by geometry and position variation of the different elements, and they were studied based on aerodynamic performance and the propeller propulsive efficiency. Besides the clear effect of the propeller streamwise position above the wing, the spacing between the disc and the main wing's surface has a direct effect on the wing pressure distribution. Therefore also this tip clearance effect was considered in the aerodynamic analysis.

Fig. 10 shows a cross sectional drawing of the CFD model, the model geometrical parameters and the orientation of each element in an OTW configuration. The position of the propeller with respect to the main wing and the secondary wing affects the overall performance of this model significantly. However, varying the location of the disc complicated the optimization study due to unwanted mesh deformations that detrimentally influenced the CFD solutions. Therefore, the influence of propeller's position on the system's efficiency was investigated separately.

The main wing airfoil was chosen based on the ATR72 turboprop aircraft, which is close to a standard NACA43015 [14] . However, this airfoil produces large pressure gradients, which could cause flow

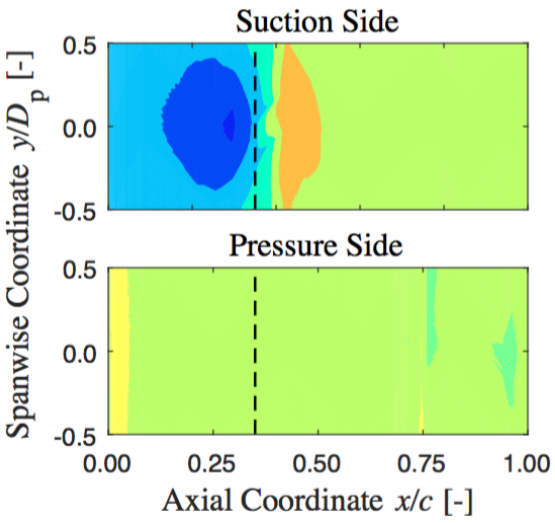

Figure 4 Upper and lower side pressure distribution for Test #2. Propeller at x/c=0.35 above an NLF422 wing (dashed line). Data taken from Markus et al [13].

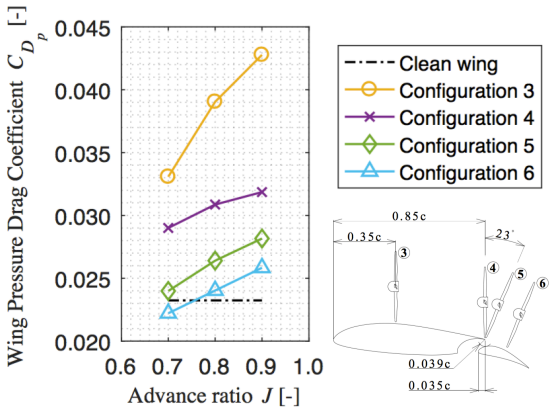

Figure 5 Example of an over the wing propeller on the wing pressure drag as found by Markus et al [13]. The propeller was positioned at several streamwise locations.

recirculation in non-optimized configurations [21]. Therefore, it was decided to move the camber location of the airfoil from 15% chordwise position to 40% to decrease such effects. The secondary wing is a new element added to the OTW based propeller model. The chord length of the secondary wing was selected between 30% to 40% of the main wing's chord length in line with the study performed by Hongbo et al [15]. Moreover, the secondary wing's chord length range was limited to prevent degraded mesh quality in the optimization study [21].

To determine the power that each of the DP-propellers would deliver it is assumed that the required propulsive power of the ATR72 reference aircraft is distributed over three different propulsion systems, namely: a) the over the wing based DP system, b) tip propellers, and c) a tail propulsion system (propulsive empennage). The array of engines is assumed to be distributed over 50% of the wingspan minus the width of the fuselage. This led to a minimum gap between the main and and the secondary wing of 0.68m, which is equal to 30% of the local wing chord. The assumptions above are to specify the initial point of the design, and the accuracy of the assumptions in this particular case will not affect the final analysis.

B. Actuator disk model and power estimation

Complex aerodynamic interaction between propeller blades and the wing could make the simulation's convergence problematic. However, earlier studies have indicated the time averaged propulsive efficiency is hardly effected. Hence, in this study, the propeller was represented by an actuator disc model. According to Stevens et al [16], such model can significantly reduce the computational cost of simulations and still generate accurate solutions. The exerted momentum in axial and tangential directions is calculated by a blade element method (BEM) solver and the resultant forces are distributed over a momentum source subdomain, where the propeller is located. The variation of propeller's inlet flow velocity due to propeller wing interaction determines the influence of body elements on the propeller's performance.

This study assumes that one third of the reference aircraft engine power is distributed over the model's wingspan. The power of each engine in the array was obtained by dividing the engine power by the number of the engines distributed over the wingspan. The propeller diameter is restricted by the wing part where the

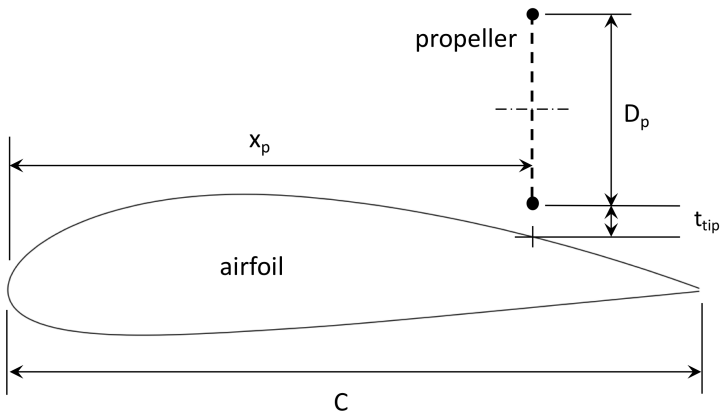

Figure 6 Key geometrical parameters related to a propeller wing configuration in a typical OTW layout.

Table 1 Propeller specifications and parameters are based on a Hamilton standard 568F propeller as used in this study.

Parameter	Value
Number of blades	6
Speed	$10,000 RPM$
Diameter	$0.5m$
Free-stream velocity	$135m/s$
Power	$34.2kW$

distributed propulsion system is placed, which is roughly 6 meters long. Assuming that there are ten engines placed over the wingspan with a lateral clearance of 20% of the propeller diameter, the propeller's diameter is estimated to be 0.5 meters.

The propeller clearance is chosen based on NASA distributed propulsion vertical take-off and landing (VTOL) tilt wing aircraft model GL10 [17]. The GL10 scaled model for wind tunnel testing uses eight propellers with 9 inches of diameter placed over a wing with 126 inches of wingspan. The spacing between the propeller's tips is variable and between 20% to 38% of the propeller diameter.

The propeller inflow velocity is initially set equal to the free-stream velocity, which is chosen based on ATR72's cruise condition. It is reasonable to assume that only 50% of the engine's full power is required during cruise condition. Hence, as Table 1 shows, each engine requires about 34.2 [kW] of power. Based on the given propeller diameter and cruise power required, the propeller characteristics were calculated using a Blade Element Method (BEM) solver.

The propeller is modeled through an actuator disc approach where the thrust and torque are modeled by assuming that the momentum is introduced over a finite thickness to reduce grid dependency that is normally found for infinitesimally thin disks [19].

C. Euler model

In this study Euler analyses are performed using the commercial flow solver ANSYS CFX. Although the Euler method does not capture the viscous effects like free stream turbulence and the boundary layer, it is

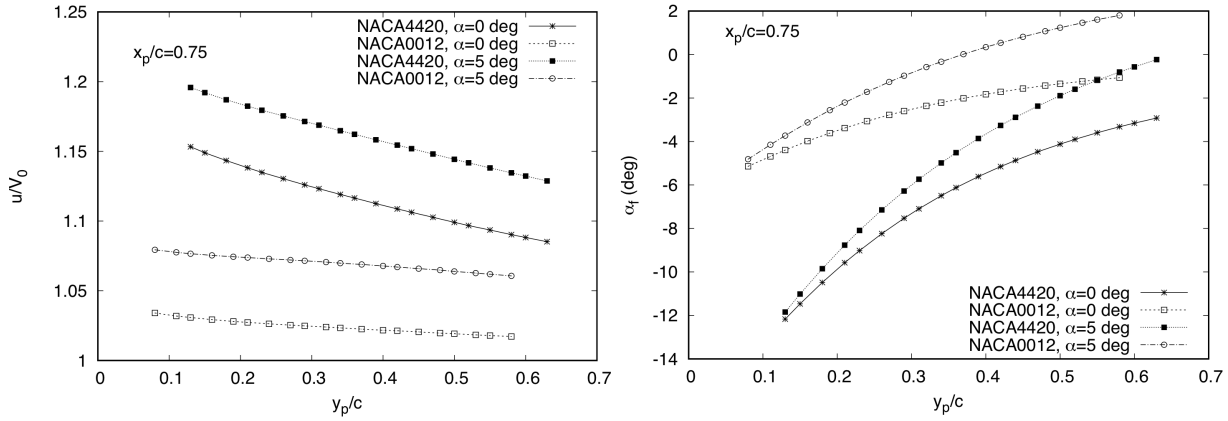

(b)

Figure 7 Effect of wing induced wing induced flow field on the local axial flow speed, u, (left) and the flow angle of attack, α_f (right), in the propeller plane for 2 different airfoils at angles of attack of $\alpha = 0^0$ and 5^0; y_p/c is the relative distance above wing in the propeller plane. Velocity data were obtained from a 2D potential airfoil flow solver for a reference undisturbed flow speed of V_0.

proven to be helpful in studying the fluid dynamics problem and interactions between multiple elements[20]. Applying RANS models and trying to capture viscous effects, the simulations were considered to become overly expensive and to complicated for this initial design study. Furthermore modeling and meshing become more problematic as the complexity of the simulation increases. The number and the orientation of the cells to capture the flow's boundary layer could become a serious issue while performing a grid convergence study to quantify the discretization error. In addition, RANS models have substantial modeling error because they are based on experimental data and correlations. Muller et al[10] and Hongbo et al[15] used RANS calculations in their studies. In their case, the number of simulations was limited so they could construct and execute costlier calculations. This study aims at investigating the influence of different parameters on the aerodynamic performance of the model, which requires numerous sets of simulations. The intrinsic assumptions in applying the Euler equations is that the boundary layer remains attached and its displacement thickness plays a negligible role in changes to the field field that the wing exerts on the propeller. Given the high Re-number at which the reference aircraft operates in cruise condition, with flaps retracted, these assumptions are regarded valid.

D. Numerical analysis and optimization setup

The influence of multiple parameters on aerodynamic performance and overall propulsive efficiency of the system was studied. For this purpose the spacing between the wings, secondary wing shape, secondary wing angle of attack and the camber position of the main wing were varied. The primary goal of these studies was to recognize the key parameters that influence propeller wing interaction when a secondary wing was added to over-the-wing propulsion system, as suggested by Hongbo et al [15]. Moreover, these preliminary results were utilized to obtain an initiation point for the later optimization study which helps to prevent an unnecessary high number of iterations to reach an optimum. The influence of wings on the propeller's inlet flow velocity and the propeller's performance was included by iteratively obtaining the inlet flow velocity of the propeller from CFD simulations and calculating the propeller's characteristics with the help of BEM calculations.

The procedure of the optimization is simplified as much as possible to construct an inexpensive algorithm. If the velocity and pressure gradients were not controlled, they could produce unpredictable flow features

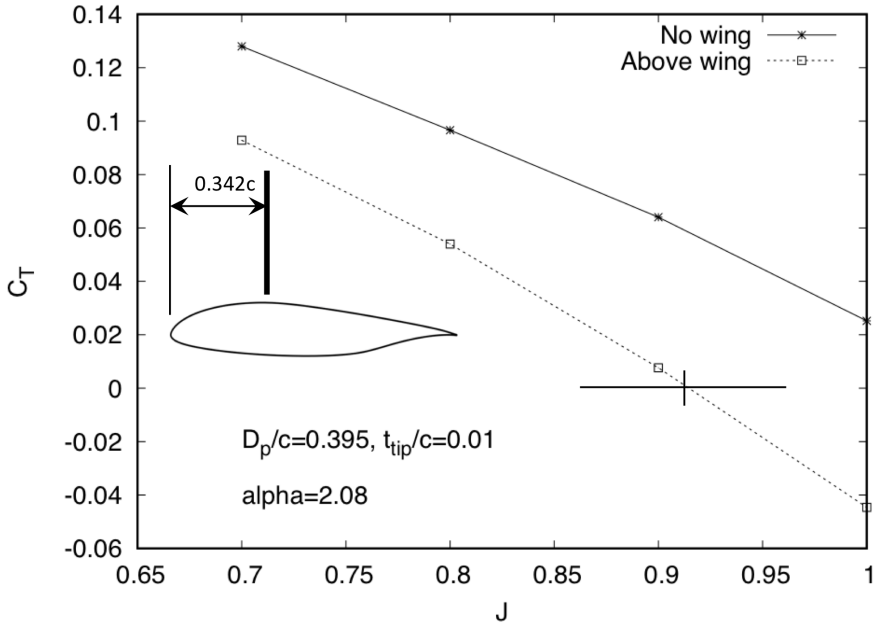

Figure 8 Example of wing effect on the OTW propeller thrust coefficient, C_T, based on a combined blade element model and surface singularity method. The model consists of a 4-bladed propeller and NLF-Mod-22B airfoil as applied by Marcus et al [13]. Wing angle of attack is $\alpha = 2.08^0$.

such as strong vortices. The drag coefficient of the system directly correlates with the velocity gradients of the flow according to Muller et al[9, 10]. It is recommended not to increase the drag coefficient of the wingless aircraft so that the optimizer chooses to decrease the drag coefficient of the system. If the optimizer chooses to increase the lift coefficient of the objective function instead of decreasing the drag coefficient, the shape of the wing may get modified in a way that the velocity gradients increase and the simulations become unstable due to flow recirculation. However, considering this parameter alone could lead to a configuration with low lifting performance, because the value of the drag coefficient relates to the system's lifting performance as well. Therefore, it is decided to maximize the lift to drag ratio of the model with a suitable drag coefficient of the wingless aircraft value. The overall propulsive efficiency is also included in the objective function. Although, the propeller thrust is considered constant, the drag force included in the overall propulsive efficiency influences the objective function of this optimization. The total lift and drag

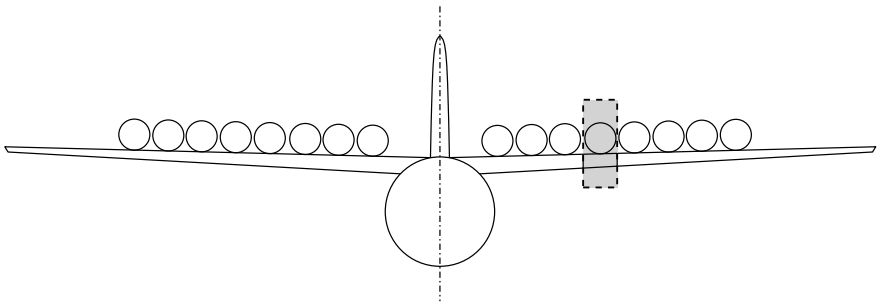

Figure 9 Front view of the model considered in the numerical study. The gray area is part of a hypothetical distributed propulsion system applied on a reference turboprop aircraft (ATR72).

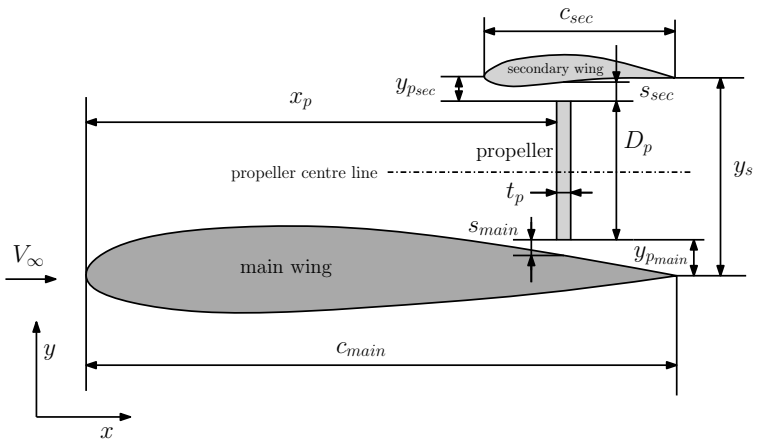

Figure 10 Sketch of the CFD model cross-sectional geometry showing the relevant shape and propeller position parameters.

coefficient of the system are defined as:

$$C_{L_{tot}} = \frac{F_{y_{main}} + F_{y_{sec}}}{q_\infty S_{ref}} \tag{1}$$

$$C_{D_{tot}} = \frac{F_{x_{main}} + F_{x_{sec}}}{q_\infty S_{ref}} \tag{2}$$

where F_x and F_y are the overall force forces acting on the main (index *main*) and secondary wing (index $sec.$). The main wing surface area, S_{ref}, is used as the reference area.

The lift to drag area as defined in eq. 3 is considered for this analysis. The parameter $C_{D_{ATR72}}$ is the drag coefficient of the wingless ATR72 aircraft. This component, taken from Nita et al[14], is estimated to be equal to 0.01107 by only including drag of the fuselage, the vertical and the horizontal tail. Hence:

$$\frac{L}{D} = \frac{C_{L_{tot}}}{C_{D_{tot}} + C_{D_{ATR72}}} \tag{3}$$

Eq. (4) shows the definition of the overall propulsive efficiency of the system. It depends on the sum of the axial forces acting on the system including the main wing and secondary wing's drag and the propeller's thrust:

$$\eta_{pp} = \frac{-V_\infty \cdot F_x}{P} = \frac{-V_\infty (D_{main} + D_{sec} - T)}{P} \tag{4}$$

The objective function of the optimization study is defined as:

$$I = \frac{1}{2}\left(\frac{\frac{C_L}{C_D + C_{D_{ATR72}}}}{\frac{C_{L_0}}{C_{D_0} + C_{D_{ATR72}}}} + \frac{\eta_{pp}}{\eta_{pp_0}} \right)$$

where index 0 refers to the initial values. It is to maximize the aerodynamic performance and the overall propulsive efficiency. Considering the overall propulsive efficiency in the objective function it incorporates the effect of wings on the propeller's inflow velocity. The flow accelerates over the upper surface of the main wing and reduces the thrust produced by the propeller according to BEM calculation. Therefore, maximizing the propulsive efficiency would mean minimizing the drag produced by the wing and optimizing the duct shape to reduce the propeller's inflow velocity.

Table 2 Specification of parameters applied in the preliminary model study.

Parameter	Value
Main wing airfoil	NACA0012
Secondary wing airfoil	NACA0012
Main wing Chord length, C_{main}	2.11[m]
Secondary wing chord length	30% C_{main}
Main wing's angle of attack	0^0
Spacing between the wings, y_s	40% C_{main}
Disc Diameter	$0.5m$
Disc position, x	$100\%C_{main}$
Thrust	$650N$
Free-stream Mach number	0.2
Calculation type	inviscid flow
Disc center position, $y_{p_{main}} + \frac{D_p}{2}$	$20\%C_{main}$

IV. Results

A. Preliminary model analysis

To obtain a general understanding of the interaction effects a preliminary analysis was performed using symmetrical airfoil sections. In this way the main effects are more easily interpretable as symmetrical airfoils sections under zero angle of attack are expected to produce zero lift and equal pressure distribution on upper and lower side. The primary focus of this part of the study was to appreciate the impact of propeller and secondary wing on the main wing and also the effect of secondary wing on the system's overall performance. Table 2 summarizes the model description used for this analysis.

Fig. 11a shows the difference in the pressure coefficient between the upper and lower surface of the main wing under the influence of the disc and the secondary wing. These interactions have a positive effect by increasing the dynamic pressure over the upper surface of the main wing which leads to positive lift.

Fig. 11b shows that the main influence on the main wing comes from the secondary element as it tends to increase the flow velocity over the upper side. The space between the main wing and the secondary wing behaves similarly to a converging-diverging nozzle which increases the flow velocity upstream of the secondary wing until the flow reaches the nozzle's throat after which pressure recovery occurs.

An opposite effect occurs when the pressure distribution on the secondary wing is considered. Fig. 12 shows that the lift coefficient of the secondary wing is negative. It is evident that the bottom surface of the secondary wing experiences higher suction than the top surface due to the interaction between the disc and the secondary wing. Furthermore it is clear that the propeller is only aggravating this strong effect on the pressure distribution. The spacing between the wings acts similar to a converging-diverging nozzle, which is confirmed by investigating the pressure coefficient of the secondary wing without the presence of the propeller. The flow velocity increases rapidly at the leading edge of the secondary wing because the area between the wings suddenly decreases. However, the flow velocity starts to decreases as the space between the wings increases.

Prior to optimizing the model geometry the effect of the spacing between the wings was studied since it is clear that the duct between the main wing and the secondary wing significantly influences the overall performance. The spacing between the main wing and the disc was chosen constant and kept small to increase

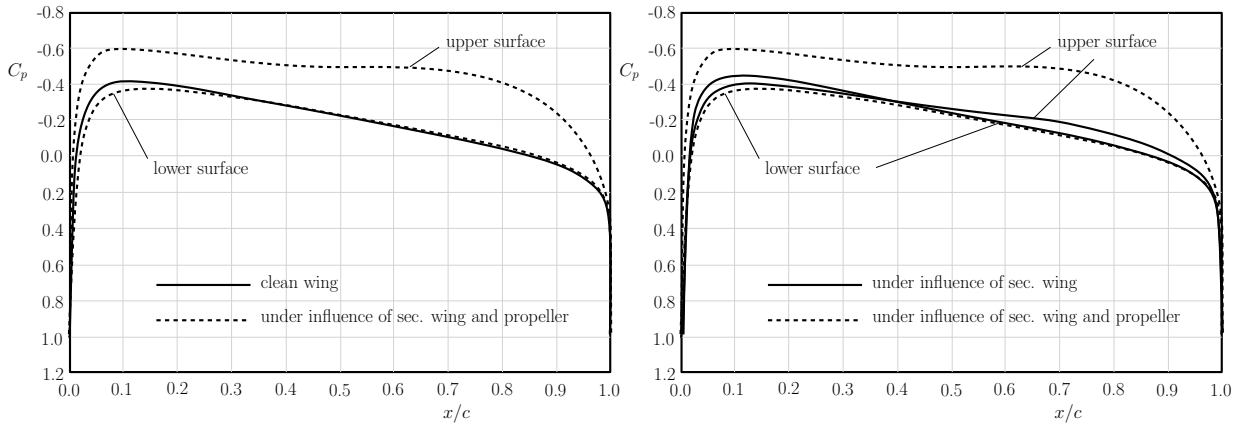

(b)

Figure 11 Pressure coefficient of the main wing with and without the influence of the propeller and the secondary wing, at 50% spanwise position of a NACA0012 airfoil model.

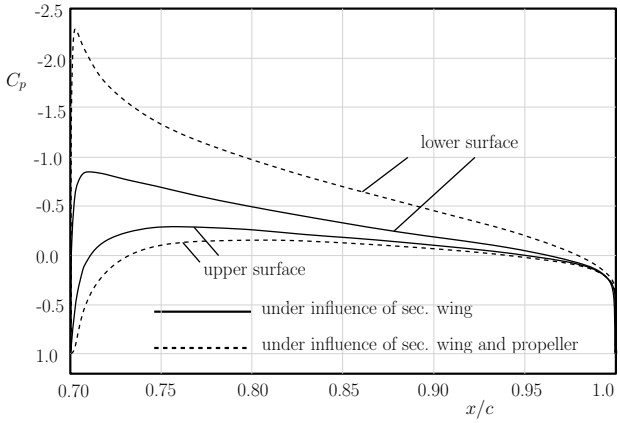

Figure 12 Pressure coefficient of the secondary wing with and without the influence of the propeller.

propeller wing interaction ($s_{main}/D_p = 0.03$). The main airfoil that was used in this study is a NACA48015 as this shape is close to the ATR72 reference case that was used in the optimization study.

Fig. 13(a) and (b) show an increase in total lift coefficient as the spacing between the wings was increased which is attributed to an increase in the main wing lift coefficient and a decrease in the negative lift on the secondary wing. This study shows that the interaction between the propeller and the secondary wing has more influence on the system's lifting performance than the interactions between the main wing and the secondary wing. Hence a shape optimization of the latter is expected to improve the overall lift performance of the model.

Fig. 13(c) and (d) show the behavior of the drag force as the spacing between the wings increases. In this case, the pressure drag due to propeller wing interaction was calculated by the integral of pressure forces acting on the surface of the wing parallel to the flow direction. The total drag coefficient increased as the spacing between wings was increased which also influences the overall propulsive efficiency because it changes the total axial force component acting on the model. It is important to realize that the drag coefficient of the secondary wing increased as the lift coefficient was improved, which could indicate that the pressure drag due to interactions is also lift dependent and it exists because of the propeller.

The aerodynamic performance and the propulsive efficiency showed high sensitivity to the shape of the

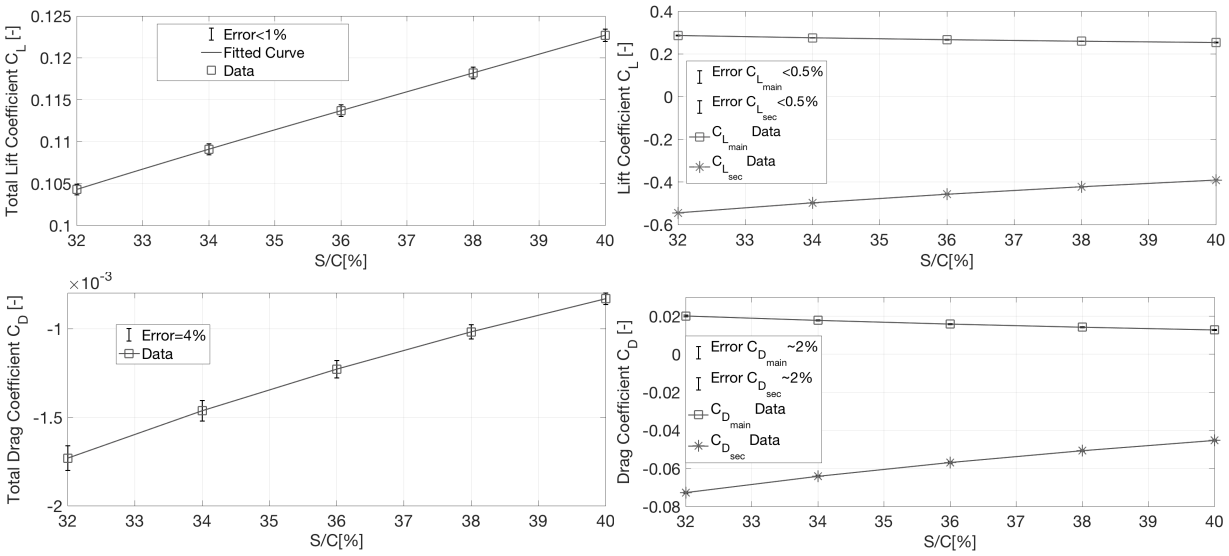

Figure 13 Effect of the wing spacing on the lift coefficient. Main and secondary wing NACA48015, $c_{main} = 2.11m$**,** $c_{sec}/c_{main} = 0.3$**,** $\alpha_{main} = \alpha_{sec} = 0^0$**,** $D_p/c_{main} = 0.234$**,** $x/c_{main} = 0.85$**,** $T = 250N$**,** $M_\infty = 0.41$**.**

secondary wing. This element affects the flow upstream of the disc, and its lower surface is significantly affected by propeller interaction. Decreasing the flow velocity by increasing the static pressure in this region could help improve the overall aerodynamic performance. Moreover, decreasing the velocity in the duct could increase the thrust force of propeller, and as a result, an optimum shape of the secondary wing would improve overall propulsive efficiency. The dominating influence of the secondary wing on the system's performance was confirmed also by investigating the effect of changes to its lift behaviour through modification of the airfoil camber and the angle of attack.

Instead of looking at the lift and drag behaviour separately, the objective function, J, as presented in Fig. 13, draws a clear picture of the effect of the changing the initial lift coefficient of the secondary wing. In this study the system's propulsive efficiency and aerodynamic performance were weighted equally, which increased the dependency of the objective function more on the aerodynamic performance factor, since the order of lift to drag ratio's variation was higher than the propulsive efficiency.

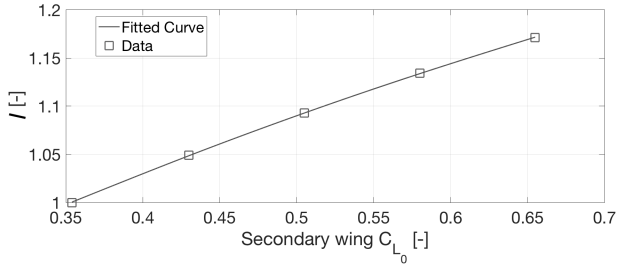

Figure 14 The objective function, J**, as a function of the secondary wing's lift coefficient,** C_{L_0}**. The influence of the propulsive efficiency was added in the calculations.**

Table 3 Initial and optimized model parameters of the secondary wing shape and disc position optimization study performed with adiabatic flow condition and constant thrust assumption for the propeller. Main design parameters: $c_{main} = 2.11m$**,** $c_{sec}/c_{main} = 0.324$**,** $D_p/c_{main} = 0.234$**,** $x/c_{main} = 0.825$**,** $T = 250N$**,** $M_\infty = 0.41$**.**

Parameter	Initial value	Optimized value	Normalized
$C_{L_{tot}}$	0.3797	0.3551	0.935
$C_{D_{tot}}$	0.00135	0.000298	0.221
η_{prop}	0.8929	0.8949	1.002
η_{pp}	0.8217	0.8712	1.060
Obj. value, J	1	1.041	-
Main airfoil	NACA48015	NACA48015	
Sec. airfoil	NACA 63A-515	Optimized Airfoil	

B. Optimized model

To obtain an improved wing and propeller model the optimization procedure, that was outlined in section III.D was applied. In this case the propeller thrust coefficient was maintain at a constant value. For a detailed description of the optimization and solvers execution sequence the reader is referred to [21].

1. Secondary wing shape optimization

The analyses in section IV.A showed that the effect of the secondary wing on the system's overall performance is significant. Moreover, the shape of the secondary wing alters the flow velocity and its distribution that the propeller experiences. To allow an optimization of the secondary wing geometry its shape was parametrized with the use of twelve CST coefficients.

The result of this design optimization is presented in Table 3 the total drag coefficient decreased substantially compared to the lift coefficient.

The objective function of the optimization included the drag coefficient of the wingless aircraft. However, the objective function remained sensitive to the variation of drag coefficient. Therefore, the optimizer chose to minimize drag coefficient instead of maximizing lift coefficient. Since the optimization was done under the assumption of constant thrust, the propeller's thrust was not affected by the variation of the inlet flow velocity, and therefore a high value of propulsive efficiency was achieved. This optimization resulted in a secondary wing shape that reduced the total drag coefficient by reducing flow acceleration upstream the converging part of the duct.

In Fig. 15 the initial and the optimized secondary wing airfoils are presented. Apparently, the thickness and the chord length of the secondary wing decreases slightly to reduce the pressure drag due to propeller wing interaction. Moreover, the nose radius of the airfoil is also decreased to reduce the suction peak. These changes lead to a lower acceleration of the flow and as result lower drag coefficient.

It should be noted that this optimization study was conducted with isothermal flow condition and after the optimum point of the optimization was reached, the initial and optimized point were simulated with adiabatic flow conditions. Performing the optimization study with isothermal flow condition reduced the computational cost of the optimization by half. However, it seems that such assumption might be inaccurate

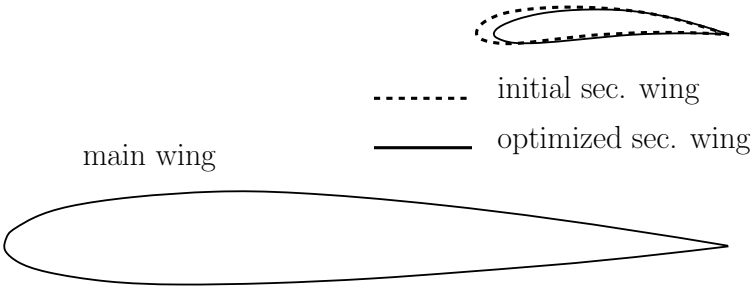

Figure 15 Cross sectional shape of the initial and optimized model.

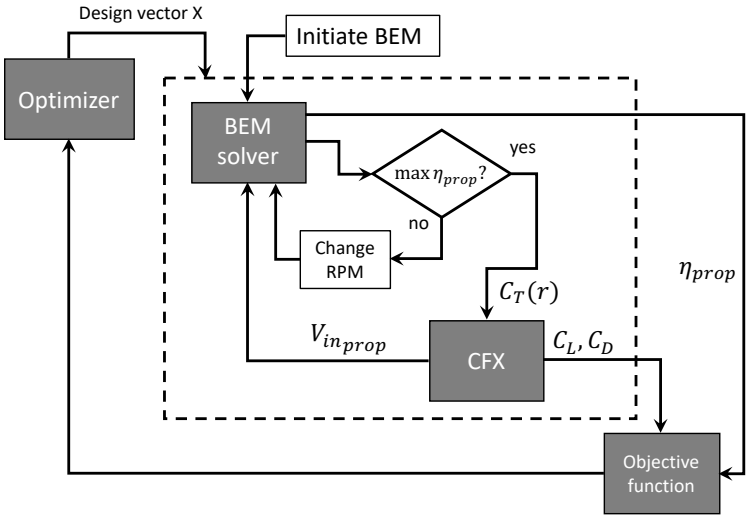

Figure 16 Overview of multi-parameter optimization procedure taking into account optimum propeller performance by adapting propeller inflow and propeller speed.

when the objective of the optimization is to minimize the drag coefficient as this coefficient is particularly affected by entropy production that is associated with potential changes in the drag coefficients. Details on the difference between isothermal and adiabatic flow conditions are described in more detail in [21].

2. Multi-parameter performance optimization

In the last part of the optimization study a multi-parameter optimization was performed in which the effect of parameters and variables that defined both the geometry and the position of the secondary wing were investigated.

Fig. 16 illustrates the algorithm of the implemented optimization procedure, which includes the effect of the inlet flow velocity on the propeller. In this case, besides the solver CFX, the call to the BEM solver was implemented required to calculate and alter the propeller's performance due to changes to the inlet velocity.

In this study, the secondary wing's shape and chord length and the spacing between the wings were subjected to optimization to increase the system's aerodynamic performance and propulsive efficiency. The airfoil shape of the secondary wing was defined by twelve CST coefficients. The spacing between the wings was defined as the distance between the chord lines of the wings normalized by the main wing chord length. The mesh flexibility and requirements bounded the design vector elements. The maximum upper and lower bound were chosen not to interfere with the mesh construction and also not to produce unwanted mesh deformities that could influence the discretization error of the model.

The last four elements of the 14-element design vector (12 CST coefficients, secondary wing chord length and wing spacing) increased up to the maximum possible bound which means that the results of this study, unfortunately, do not yet represent a global maximum value of the objective function[21]. As in this part of the study the aim was to maximize the lifting performance of the model the drag coefficient of the ATR72 aircraft was increased to reduce the sensitivity of the objective function to the drag coefficient. Its value was chosen from [14], and set equal to 0.0274. In this case the total drag coefficient of the wingless aircraft was considered by including the effect of the engine casing and nacelle and the zero-lift drag coefficient of the wing.

As Fig. 17 shows, the overall thickness of the secondary wing, the chord length and the spacing between the wings were increased. Like found in the earlier test cases, the spacing between the wings was increased leading to an improvement of the system's lift. The optimized airfoil shows a small overall thickness growth. However, a noticeable improvement in the optimized airfoil was that the thickness of the airfoil's rear upper surface was increased.

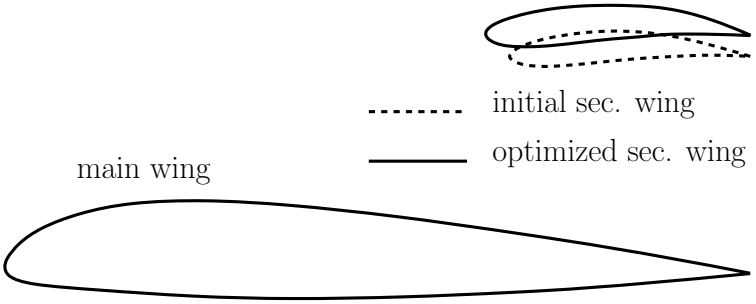

Figure 17 2D plot of the initial and optimized model.

As the Table 4 shows, the optimizer chose to increase the lift coefficient over the drag coefficient. The initial point of the optimization would typically represent an ATR72 aircraft based on the proposed distributed propulsion system with the addition of a secondary wing element.

Table 4 Initial and optimized model parameter values of the study in which secondary wing shape and chord and distance between the wings were optimized. Main design parameters: $c_{main} = 2.11m$**,** $D_p/c_{main} = 0.234$**,** $x/c_{main} = 0.825$**,** $M_\infty = 0.41$**. Parameter** $V_{prop_{in}}$ **is the average inflow speed over the propeller disk. Adiabatic flow condition**

Parameter	Initial value	Optimized value	Normalized
$C_{L_{tot}}$	0.559612	0.660661	1.1805
$C_{D_{tot}}$	0.00083	0.00182	2.1941
η_{prop}	0.9042	0.9093	1.005
η_{pp}	0.6960	0.705	1.012
Obj. value, J	1	1.073	-
V_∞/nD_p	1.925	1.2	0.6234
$V_{prop_{in}}$	$161.6m/s$	$154.7m/s$	0.9573
$T(N)$	209	220	1.052

This design optimization was meant to include propeller's inflow velocity effects in the optimization study. By including a BEM based discipline in the optimization routine the propeller's performance was improved based on the inlet flow velocity. Moreover, this study was meant to optimize the lift characteristics of the system by restraining the pressure drag influence on the model. The overall thickness of the secondary wing was increased by the optimizer which was contradictory to the results of the study where the system's drag behavior was dominant. It is interesting to observe that even though the drag coefficient of the system was significantly increased, the overall propulsive efficiency of system was maintained due to the influence of wings on propeller's performance. This study shows, that by increasing the lift coefficient of the secondary wing, the flow velocity in the duct decreased, which increased the generated thrust force by the propeller and as result the overall propulsive efficiency was maintained.

V. Conclusions & Outlook

From this preliminary numerical analysis of the over-the-wing propulsion system that consisted of a wing-propeller-secondary wing configuration the following main conclusions can be drawn:

- Significant effects due to the main and secondary wing induced flow field on the OTW propeller are found. Moreover, non-uniform effects on the propeller need to be alleviated by proper duct design.
- Changes to the shape of a secondary wing, that acts as a duct, proved to have a significant effect on both the lift of the main wing and the propulsive efficiency of the propeller.
- The study shows that the combination of an Euler equations based optimization framework, that is validated with dedicated propeller-wing interaction studies, delivers feasible designs that may be employed in design studies on novel trailing edge based distributed propulsion concepts. However, from earlier studies it is known that under certain conditions (i.e. high thrust coefficients as used in take-off) flow separation may occur [10, 13]. This is especially the case where a nearby flap is deployed. Under these conditions viscous flow calculations combined with experimental analysis is required to prevent unwanted flow characteristics.
- Although the study on trailing edge based propulsion systems was quite limited so-far, the system seems to offer an efficient solution for a (hybrid-electric) propulsion design demonstrating high lift over drag ratio and high propulsive efficiency when the duct shape is properly optimized.

The data obtained in this research will be utilized to develop novel aircraft design based on TESP based distributed propulsion in which both the duct and the wing with high lift system will be optimized both with respect to shape and construction to combine high cruise propulsive efficiency with improved high lift capability. Enhanced design studies will be supported by detailed experimental studies that focus on interaction between the main wing boundary layer and the propeller.

References

[1] N.K. Borer, M.D. Patterson, J.K. Viken, M.D. Moore, J. Bevirt, A.M. Stoll, and A.R. Gibson, Design and Performance of the NASA SCEPTOR Distributed Electric Propulsion Flight Demonstrator, AIAA 2016-3920, 2016

[2] M. Ridel, B. Paluch, C. Doll, D. Donjat, J. Hermetz, et al., A Concept Plane using electric distributed propulsion Evaluation of advanced power architecture. More Electric Aircraft - MEA 2015, Feb 2015, TOULOUSE, France.

[3] A.M. Stoll, J. Bevirt, M.D. Moore, W.J. Fredericks, N.K. Borer, Drag Reduction Through Distributed Electric Propulsion, AIAA 2014-2851, 2014

[4] B. Della Corte, T. Sinnige, R. de Vries, F. Avallone, D. Ragni, G. Eitelberg, and L. Veldhuis, Tractor Propeller-Pylon Interaction, Part II: Mitigation of Unsteady Pylon Loading by Application of Leading-Edge Porosity, AIAA 2017-1176, 2017

[5] M.F.M. Hoogreef, R. Vos, R. de Vries and L.L.M. Veldhuis, Conceptual Assessment of Hybrid Electric Aircraft with Distributed Propulsion and Boosted Turbofans, AIAA 2019-1807, 2019

[6] A. Isyanov, A. Lukovnikov, A. Mirzoyan, Development challenges of distributive propulsion systems for advanced aeroplanes, Aircraft Engineering and Aerospace Technology, Vol. 86 Issue: 6, pp.459-463, 2014

[7] K. Reynolds, N. Nguyen, E. Ting, J. Urnes Sr, Wing shaping concepts using distributed propulsion", Aircraft Engineering and Aerospace Technology, Vol. 86 Issue: 6, pp.478-482, 2014

[8] On the Effects of an Installed Propeller Slipstream on Wing Aerodynamic Characteristics, Acta Polytechnica, Vol 44, No. 3 (2004)

[9] L. Müller, D. Kozulovic, M. Hepperle, and R. Radespiel, Installation Effects of a Propeller Over a Wing with Internally Blown Flap, AIAA2012-3335, 30th AIAA Applied Aerodynamics Conference, Fluid Dynamics and Co-located Conferences, 2012

[10] L. Müller, W. Heinze, D. Kožulović, M. Hepperle, and R. Radespiel, Aerodynamic Installation Effects of an Over-the-Wing Propeller on a High-Lift Configuration, Journal of Aircraft, Vol. 51, No. 1 (2014), pp. 249-258.

[11] A.P.M Luijendijk, Propeller-wing interference study for over the wing positioned propeller configuration, MSc Thesis, Delft University of Technology, Faculty of Aerospace Engineering, 2002.

[12] L.L.M. Veldhuis, Propeller Wing Aerodynamic Interference, PhD dissertation, Delft University of Technology, 2005.

[13] E.A. Marcus, R. de Vries, A. Raju Kulkarni, and L.L.M. Veldhuis, Aerodynamic Investigation of an Over-the-Wing Propeller for Distributed Propulsion, 2018 AIAA Aerospace Sciences Meeting, AIAA SciTech Forum, AIAA 2018-2053

[14] M. F. Nita, D. Scholz, Aircraft Design Studies Based on the ATR72, Department of Automotive and Aeronautical Engineering, Hamburg University of Applied Sciences, 2008

[15] W. Hongbo, Z. Xiaoping, Z. Zhou, Numerical simulation of the propeller/wing interactions at low Reynolds number, School of Aeronautics and Science and technology in UAV Laboratory, Northwestern Polytechnic University Xi'an, China, 2016

[16] R.J.A.M. Stevens, L.A. Martínez-Tossas, C. Meneveau, Comparison of wind farm large eddy simulations using actuator disk and actuator line models with wind tunnel experiments", Department of Physics, Mesa Institute, and J. M. Burgers Centre for Fluid Dynamics, University of Twente, Department of Mechanical Engineering & Center for Environmental and Applied Fluid Mechanics, Johns Hopkins University, 2016

[17] P. M. Rothhaar, P. C. Murphy, B. J. Bacon, I. M. Gregory, J. A. Grauer, R. C. Busan, and M. A. Croom, NASA Langley Distributed Propulsion VTOL Tilt-Wing Aircraft Testing, Modeling, Simulation, Control, and Flight Test Development, NASA Langley Research Center, Hampton, Virginia, 23681

[18] A. Seitz, J. Bijewitz, S. Kaiser, G. Wortmann, Conceptual investigation of a propulsive fuselage aircraft layout, Visionary Aircraft Concepts Bauhaus Luftfahrt e.V. and Munich, Germany, Munich Aerospace e.V.Munich, Germany

[19] N. Simisiroglou, M. Karatsioris, K. Nilsson, S.P. Breton, S. Ivanell, The actuator disc concept in PHOENICS, 13th Deep Sea Offshore Wind R&D Conference, EERA DeepWind'2016, 20-22 January 2016, Trondheim, Norway

[20] K.K. Mani, Design using Euler Equations, Lockheed-California Company, Burbank, AIAA 2nd applied Aerodynamics Conference, Seattle, Washington, 1984

[21] A. Khajehzadeh, Analysis of an Over the Wing Based Distributed Propulsion System, MSc Thesis, Delft University of Technology, March 2018.